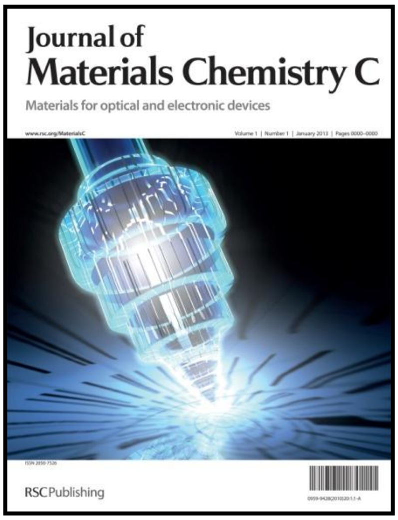

Journal of Materials Chemistry C

Materials for Optical and Electronic Devices

Full paper submission

Journal of Materials Chemistry C is a weekly journal in the materials field. The journal is interdisciplinary, publishing work of international significance on all aspects of materials chemistry related to optics and electronics. Articles cover the fabrication, properties and applications of materials.

2012 Impact Factor of *Journal of Materials Chemistry*: **6.10**
For more information go to www.rsc.org/materialsC

The following paper has been submitted to *Journal of Materials Chemistry C* for consideration as a **full paper**.

Journal of Materials Chemistry C wishes to publish original research that demonstrates **novelty and advance**, either in the chemistry used to produce materials or in the properties/applications of the materials produced. Work submitted that is outside of these criteria will not usually be considered for publication. The materials should also be related to the theme of materials for optics and electronics.

Routine or incremental work, however competently researched and reported, should not be recommended for publication if it does not meet our expectations with regard to novelty and impact.

It is the responsibility of authors to provide fully convincing evidence for the homogeneity and identity of all compounds they claim as new. Evidence of both purity and identity is required to establish that the properties and constants reported are those of the compound with the new structure claimed.

Thank you for your effort in reviewing this submission. It is only through the continued service of referees that we can maintain both the high quality of the publication and the rapid response times to authors. We would greatly appreciate if you could review this paper in **two weeks**. Please let us know if that will not be possible.

Once again, we appreciate your time in serving as a reviewer. To acknowledge this, the RSC offers a **25% discount** on its books: http://www.rsc.org/Shop/books/discounts.asp. Please also consider submitting your next manuscript to *Journal of Materials Chemistry C*.

Best wishes,

Liz Dunn
Managing Editor, *Journal of Materials Chemistry C*

Apr 18, 2014

Dear Gitti Frey,
Associate Editor of Journal of Materials Chemistry C

Re: Revision Requested for Manuscript ID TC-ART-01-2014-000101.R1

Title: "Fabrication of functional nano-sized patterns with UV-curable polysilsesquioxane on photovoltaic protective glass substrates using hybrid nano-imprint lithography"

We appreciate your valuable comments and suggestions, which have resulted in modifications that have strengthened the paper. We have revised the manuscript in accordance with the reviewer's comments and suggestions.

Attached to this letter please find the following documents:

· Our point-to-point responses to the referees' comments and suggestions,

Thank you again for your reconsideration of our manuscript.

Sincerely,

Prof. Heon Lee

Responses to Comments from Editor (Reviewers):

A list of changes as mentioned:

- The reason why we choose the hybrid organic-inorganic material was added. (We try to benefit the advantages of both organic and inorganic materials.)
- The reason why we use laser interference lithography to manufacture moth-eye structures was added.

Reviewer #3:

1. The authors fabricated photovoltaic protective glasses with nano-size patterned polysilsesquioxane moth-eye structures. Although the used polymer has superior thermal stability, hardness, and chemical durability, which are significantly important properties to use the photovoltaic devices in outdoor, compared with conventional organic materials, its properties might poor compared to the used photovoltaic protective glass itself. Hence, photovoltaic protective glasses with antireflective glass moth-eye structures have been recently explored to protect the photovoltaic devices from external environment and to improve the efficiency of photovoltaic devices [1-3]. Therefore, the authors need to mention the advantage of their approach compared to the aforementioned approach (i.e., direct fabrication of glass moth-eye structures on photovoltaic protective glass). It is crucial to show excellence of their research.

[1] L. K. Verma, et. al., Renewable Energy, 36, 2489-2493 (2011).

[2] Y. M. Song, et. al., Optics Express, 20(S6), A916-A923 (2012)

[3] J. Son, et. al., Solar Energy Materials and Solar Cells, 98, 46-51 (2012)

Response:

Thank you for reviewer's comment. As reviewer's comment, organic material has limitation of some properties compare to inorganic material. Indeed, **the resultant pattern using organic material appears more consolidated**. Besides that, **the inorganic material has superior mechanical properties**. Therefore, **we chose of the organic-inorganic hybrid material to benefit the advantages of both materials**.

2. The authors used Ni master mold fabricated by laser interference lithography and electro plating method to produce PDMS mold. However, the laser interference lithography method is not suitable for uniformly making moth-eye patterns on large-area substrate (e.g., 85×85 mm2) as well as expensive. There are several approaches to fabricate master molds for nanoimprint lithography. For instance, anodized aluminum oxide (AAO) master mold was used to uniformly fabricate wafer-scale moth-eye patterns on polymer substrate [4]. Thus, it is required that the authors mention advantages of their method compared to other methods to fabricated moth-eye patterned polymer substrate.

[4] K. Choi, et. al., Advanced Materials, 22(33), 3713-3718 (2010)

Response:

Thank you for reviewer's comment. There are various methods to manufacture moth-eye patterns such as anodized aluminum oxide (AAO) and nano-sphere lithography. Nevertheless, **we manufacture moth-eye patterns using LIL technology due to their superior anti-reflection property compare to those which were manufactured using other technologies.**

Journal Name RSCPublishing

ARTICLE

Fabrication of functional nano-sized patterns with UV-curable polysilsesquioxane on photovoltaic protective glass substrates using hybrid nano-imprint lithography

Cite this: DOI: 10.1039/x0xx00000x

Received 00th January 2012, Accepted 00th January 2012

DOI: 10.1039/x0xx00000x

www.rsc.org/

Ju-Hyeon Shin[a], Bit-Na Go[a], Hak-Jong Choi[a], Joong-Yeon Cho[a], Albert Sung Soo Lee[b], Seung Sang Hwang[b], Hyuk Jin Cha[c] and Heon Lee[a, *]

UV-curable polysilsesquioxane materials were used to incorporate moth-eye structures on photovoltaic (PV) protective glass. These patterns were formed using a hybrid nanoimprint lithography technique and annealed at 100 °C to evaporate the solvent (xylene). Compared to the bare, un-patterned PV protective glass, the PV protective glass patterned on both sides had superior optical properties. Transmittance of the PV protective glass patterned on both sides increased by up to 3.13 % and reflectance decreased by up to 3.42 %, and the transmittance was increased for all angles of incidence. Furthermore, the J_{SC} of devices with the PV protective glass patterned on both sides increased by up to 3.15 %. Finally, a monitoring system was set up to measure electricity generated by PV modules. The efficiency of the PV module with PV protective glass patterned on both sides was enhanced by up to 12.16% compared with that of the PV module with un-patterned PV protective glass.

Introduction

Following increasing concern regarding environmental pollution, green energy technologies have been suggested to replace conventional fossil fuel power generation. In particular, photovoltaic systems are being widely studied because they can convert solar energy to electricity without emitting CO_2.[1-3] Photovoltaic (PV) protective glass is used to protect solar cells from external shock;[4-5] however as a result, incident light is reflected off the surface of the glass, resulting in decreased conversion efficiencies of PV modules. Typically, anti-reflection layers are needed to minimize reflections off the surface of PV protective glass.

In this study, moth-eye structures, a type of anti-reflection structures, were formed on the surface of PV protective glass using hybrid nanoimprint lithography (H-NIL). Typically, nanoimprint lithography processes use either heating or ultra violet (UV) exposure for curing an imprint resin. The UV-curable polysilsesquioxane, used here as an imprint resin, is a photo-initiator and dissolves in xylene, and therefore, both heating and UV exposure are required to evaporate the solvent and to cure the resin. The H-NIL process, which uses both heating and UV exposure, is thus ideal to fabricate moth-eye structures using this material.

Reflection normally occurs due to a rapid change in refractive index. Moth-eye structures enable gradual changes in refractive index, which act to reduce reflection through the moth-eye effect.[6-10] To fabricate micro- and nanosized structures, many advanced lithographic techniques have been proposed, such as those involving electron beam (e-beam), X-ray, deep-ultraviolet, and immersion.[11-14] However, only nanoimprint lithography can help fabricate micro- and nanosized structures on various types of substrates through a simpler and lower-cost process.[15-18] Nanoimprint lithography is also an optimized technology to fabricate nanosized anti-reflection patterns (such as moth-eye structures) on textured PV protective glass.[19]

UV-curable, ladder-like polysilsesquioxane has been used to fabricate moth-eye patterns on PV protective glass.[20-21] Generally, UV-curable polymers are used to fabricate functional films or structures mainly due to advantages such as increased production rate and superior elastic properties.[22-23] However, conventional UV-curable polymers become weak due to heat damage and are easily discolored.[24] In this study, an organic-inorganic hybrid material was used to overcome the disadvantages of fully organic polymers. The organic-inorganic hybrid material used in this study has superior thermal stability, hardness, and chemical durability compared with conventional organic materials.[20-21] Indeed, the resultant pattern using organic material appears more consolidated. Besides that, the inorganic material has superior mechanical properties. Therefore, we chose of the organic-inorganic hybrid material to benefit the advantages of both materials.

Experimental

Preparation of PV protective glass

Figure 1. (a) Digital photograph and SEM images of PV protective glass substrates. (b) Oblique view of the flat side, (c) oblique view, and (d) cross sectional view of the textured side

The glass substrate used for this study as PV protective glass had a low iron content (less than 95 ppm). The PV protective glass had a thickness of 3 mm and was manufactured by Nuri Co., Korea. The glass had a textured inward side (facing the PV module) and a flat outward side. The textured side had mountain-shaped structures with widths and heights of 800 μm and 80 μm, respectively, forming a regular pattern. The scanning electron microscope (SEM) images shown in Figure 1 were measured using a field emission SEM (FE-SEM) manufactured by Hitachi, Japan (Hitachi S-4300).

Fabricating Ni and PDMS molds and replicating anti-reflection patterns on the PV protective glass.

Figure 2. Schematic procedure used to fabricate the PDMS mold

A polydimethylsiloxane (PDMS) mold was manufactured from a Ni master mold with moth-eye patterns.[25] The Ni master mold was fabricated using laser interference lithography (LIL) and electro-plating technologies.[26] There are various methods to manufacture moth-eye patterns such as anodized aluminum oxide (AAO)[27] and nano-sphere lithography. Nevertheless, we manufacture moth-eye patterns using LIL technology due to their superior anti-reflection property compare to those which were manufactured using other technologies. The properties of the moth-eye structures were simulated using a finite difference time domain (FDTD) system.[28] The fabricated moth-eye structure had a width of 250–300 nm and a height of 250–265 nm. PDMS was dispensed onto the Ni master mold and heat-treated at 80 °C for 3 hours to cure the PDMS. After cooling, the PDMS was detached from the Ni master mold. Figure 2 shows a schematic diagram of the procedure used to fabricate the PDMS mold.

Figure 3. Overall process used to fabricate the moth-eye patterns on PV protective glass

Figure 3 shows the overall process used to transfer the moth-eye patterns onto PV protective glass using H-NIL. A UV-curable polysilsesquioxane was coated onto the PDMS mold by spin-coating at 3,000 rpm for 30 seconds. The UV-curable polysilsesquioxane resin contained 10 wt% silsesquioxane, 5 wt% Irgacure-184 (Ciba, Switzerland), and 75 wt% xylene (Sigma Aldrich, USA). The UV-curable polysilsesquioxane coated on the PDMS mold was transferred to both the flat and textured sides of the PV protective glass, depending on the sample type.

The solvent (xylene) was evaporated by heating to 80 °C at a pressure of 5 bar for 10 min. The glass was then exposed to UV for 10 minutes to cure the polysilsesquioxane. After cooling the PDMS molds and the PV protective glass, the PDMS molds were detached from the glass substrate. To completely remove the solvent (Xylene), the moth-eye patterns were annealed in N_2. The temperature was increased from room temperature to 100°C over 1 hour, maintained there for 1 hour, and then cooled back to room temperature over 1 hour.

Results and discussion

Moth-eye patterns formed on PV protective glass.

Figure 4. SEM images of moth-eye patterns fabricated using UV curable polysilsesquioxane from (a) the flat side (sample patterned on one side), (b) the textured side (sample patterned on one side), and (c, d) the flat and textured sides, respectively for a sample patterned on both sides.

SEM images of the moth-eye patterns formed on the PV protective glass are shown in Figure 4. SEM images of the flat and textured sides of the glass samples are shown in Figures 4 (a) and (b) after patterning on only one side and Figures 4 (c) and (d) after patterning on both sides. Moth-eye patterns with cone widths of 250-350 nm were formed uniformly and with high fidelity over the entire surface of the PV protective glass.

Figure 5. AFM images of (a) the Ni master mold with moth-eye patterns and (b) the moth-eye patterns reproduced on the PV protective glass

Figure 5 shows atomic force microscope (AFM) images of the Ni master mold with moth-eye patterns and their reproduction on the PV protective glass (textured side). The moth-eye patterns on the Ni master mold have a height of 264.70 nm and a conical structure as shown Figure 5 (a). In Figure 5 (b), the moth-eye patterns on UV-curable polysilsesquioxane have a height of 233.52 nm and appear to have shapes identical to those of the Ni master mold. The moth-eye eye patterns of the Ni master mold were replicated on the textured PV protective glass with very high fidelity.

Changes in optical and electrical properties caused by moth-eye patterns.

Figure 6. Changes in (a) transmittance and (b) reflectance due to the moth-eye patterns on the PV protective glass

Figure 6 shows the changes in transmittance and reflectance caused by the presence of moth-eye patterns on the PV protective glass. The optical properties were measured using an integrating sphere spectrophotometer (Jasco V650, USA). As shown in Figure 6 (a), the transmittance was increased compared to un-patterned bare glass. At a wavelength of 400 nm, a shift of transmittance is observed, an intrinsic property of moth-eye structures used in this study.

The optical properties of the PV protective glass patterned on the flat side were superior to those from PV protective glass patterned on the textured side. Indeed, the flat side is the one exposed to light thereby the amount of incident light which passes the moth-eye patterns is greater when these are formed on the flat side rather than on the textured side, leading to enhanced optical properties.

Moreover, when moth-eye patterns were formed on both sides of the PV protective glass, the transmittance was increased by up to 3.13 %, and the reflectance decreased by up to 3.42 % compared with un-patterned glass. These results show that superior optical properties were enabled by the moth-eye patterns. The optical properties were especially enhanced in the visible spectral range (380-770 nm). Furthermore, since the refractive indices of air (n_{air}=1), UV-curable polysilsequioxane

(n_{resin}=1.52), and glass (n_{glass}=1.52) increase sequentially, the anti-reflection effect is maximized.

Figure 7. Transmittance changes in the PV protective glass at various incident angles: (a) θ=15°, (b) θ=30°, and (c) θ=45°

In reality, light is incident on PV modules at various angles, so optical properties need to be measured as a function of angle. We therefore measured the transmittance of the PV protective glasses at angles of 15°, 30°, and 45°. As shown in Figure 7, the transmittance of the moth-eye patterned PV protective glass increased at all angles with the PV protective glass patterned on both sides showing the highest values of transmittance. Total reflection can occur in PV modules when the angle of incidence is large. The results shown Figure 7 (c) are therefore noteworthy given that even at the largest angle (θ=45°), the moth-eye patterns lead to reduced reflection.

Figure 8. I-V characteristic changes due to PV protective glass with moth-eye patterns

Current-voltage (I-V) characteristics were measured using a solar simulator (WXS-220S-L2.AM1.5GMM made by WACOM, USA). The electrical properties were all measured using the same solar cell and only the PV protective glass was changed for each measurement. The current densities (J_{SC}) of all the patterned samples increased due to the enhanced optical properties of the fabricated moth-eye patterns, as shown in Figure 8. Among the patterned samples, the J_{SC} of the PV protective glass patterned on both sides was increased by up to 3.15 % relative to the un-patterned glass. This result suggests that more electron-hole pairs were generated, helping to improve the efficiency of the PV module.

A monitoring system to measure the electricity generated by the PV modules

Figure 9. (a) Comparision of the electrical properties of each PV module used in the monitoring system; each module was assembled with un-patterned glass, moth-eye patterned glass on the textured side only, patterned glass on the flat side only, and patterned glass on both sides. (b) Schematic structure of PV module with PV protective glass used in field tests.

Finally, a monitoring system (Capture Star 1000B, ONTEST, Korea) was set up to measure electricity generated by the PV modules. Before measuring the generated power, we confirmed the efficiency differences between the PV modules as shown in Figure 9 (a). Each PV modules (1~4) was assembled with un-patterned PV glass, moth-eye patterned PV glass only on the textured side, patterned PV glass only on the flat side and patterned PV glass on both sides. To obtain accurate results, the efficiencies of each PV module were normalized to PV module 1, which was assembled with un-patterned PV protective glass. Figure 9 (b) shows a schematic structure of a PV module with PV protective glass used in the monitoring system. Crystalline silicon solar cell (SC) was stacked on the printed circuit board (PCB). Subsequently, ethylene vinyl acetate (EVA) was mounted on the stacked SC/PCB and a layer of polyethylene terephthalate (PET) was used to protect the PV module. This PV module has a total size of 85 mm * 85 mm and the P_{max} of this module is 0.8 W.

Figure 10. Comparison of PV modules with moth-eye patterns: Field test on (a) 04th, (b) 05th, (c) 06th, and (d) 07th Oct. 2013.

The PV modules with various types of protective glass were installed outdoors and monitored for 4 days. Figure 10 shows the electrical power generated by each PV module over several days. Under direct irradiation (2013.10.04 – 2013.10.05; 1PM), the moth-eye effect became more effective and more light was absorbed by PV modules with moth-eye structures due to lower reflection from the surface of the protective glass. However, on cloudy days, the light was scattered more, the moth-eye anti-reflection layer became less effective, and the increase in generated power was smaller. Moth-eye anti-reflection is effective at all angles of incidence, as seen in Figure 7, and so, increases in power at the module level were higher than demonstrated by the characteristic I-V curve.

Table 1. Changes in generated electrical power due to moth-eye patterns

Details of the electricity generated at different periods are compared in Table 1. During a sunny period (2013.10.04), the total amount of power generated was enhanced by 12.16 % by the PV protective glass patterned on both sides compared with the PV module with un-patterned PV protective glass. The gain in power varied from day to day, but PV protective glasses with moth-eye patterns always generated more power than un-patterned glass.

Inserting Graphics

Figure 1. (a) Digital photograph and SEM images of PV protective glass substrates. (b) Oblique view of the flat side, (c) oblique view, and (d) cross sectional view of the textured side

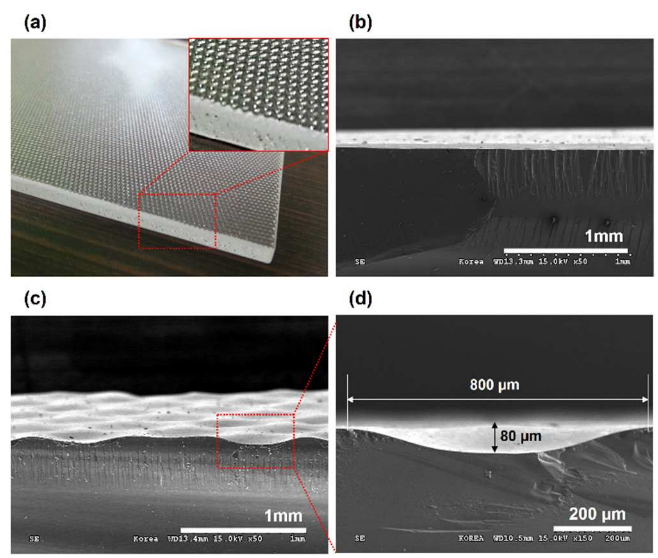

Figure 2. Schematic procedure used to fabricate the PDMS mold

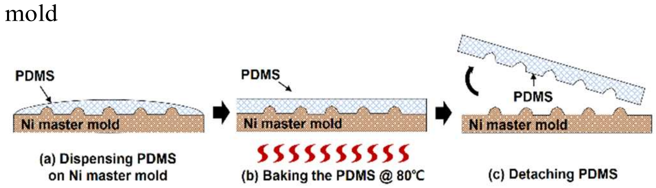

Figure 3. Overall process used to fabricate the moth-eye patterns on PV protective glass

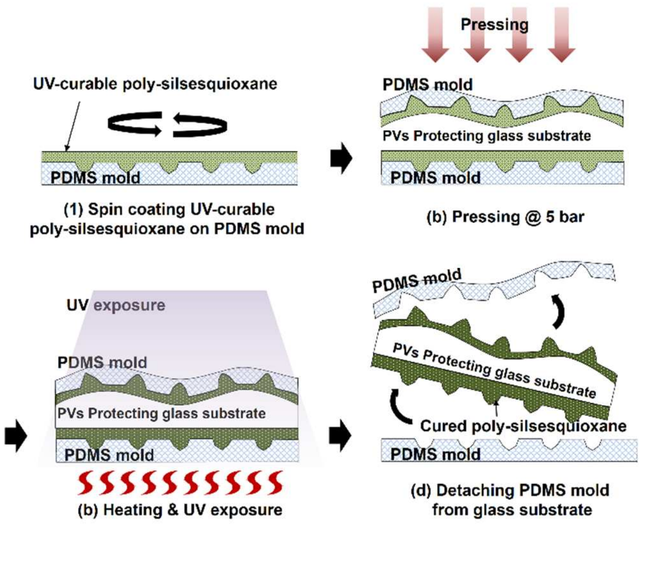

Figure 4. SEM images of moth-eye patterns fabricated using UV curable polysilsesquioxane from (a) the flat side (sample patterned on one side), (b) the textured side (sample patterned on one side), and (c, d) the flat and textured sides, respectively for a sample patterned on both sides.

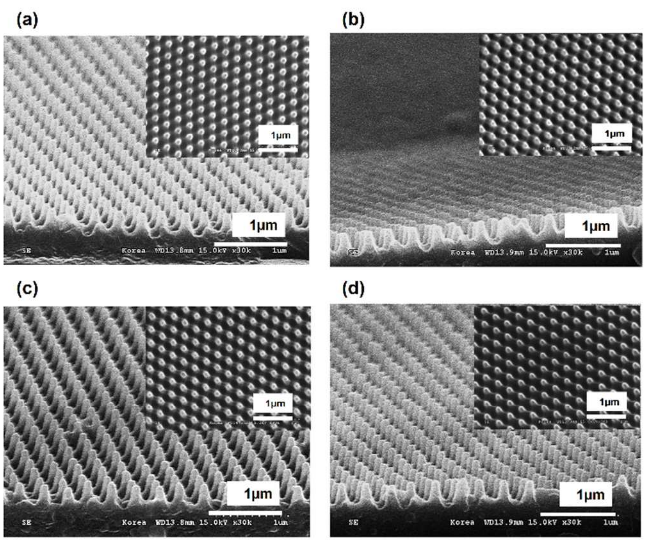

Figure 5. AFM images of (a) the Ni master mold with moth-eye patterns and (b) the moth-eye patterns reproduced on the PV protective glass

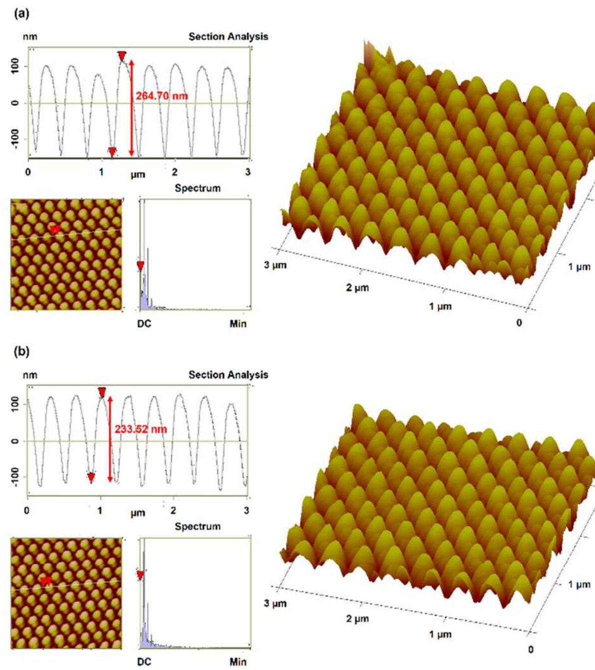

Figure 6. Changes in (a) transmittance and (b) reflectance due to the moth-eye patterns on the PV protective glass

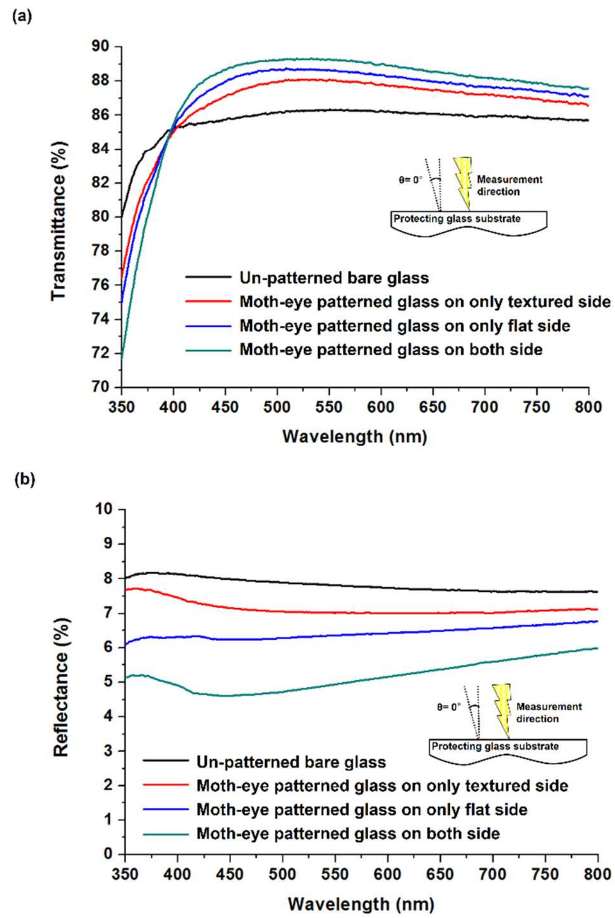

Figure 7. Transmittance changes in the PV protective glass at various incident angles: (a) θ=15°, (b) θ=30°, and (c) θ=45°

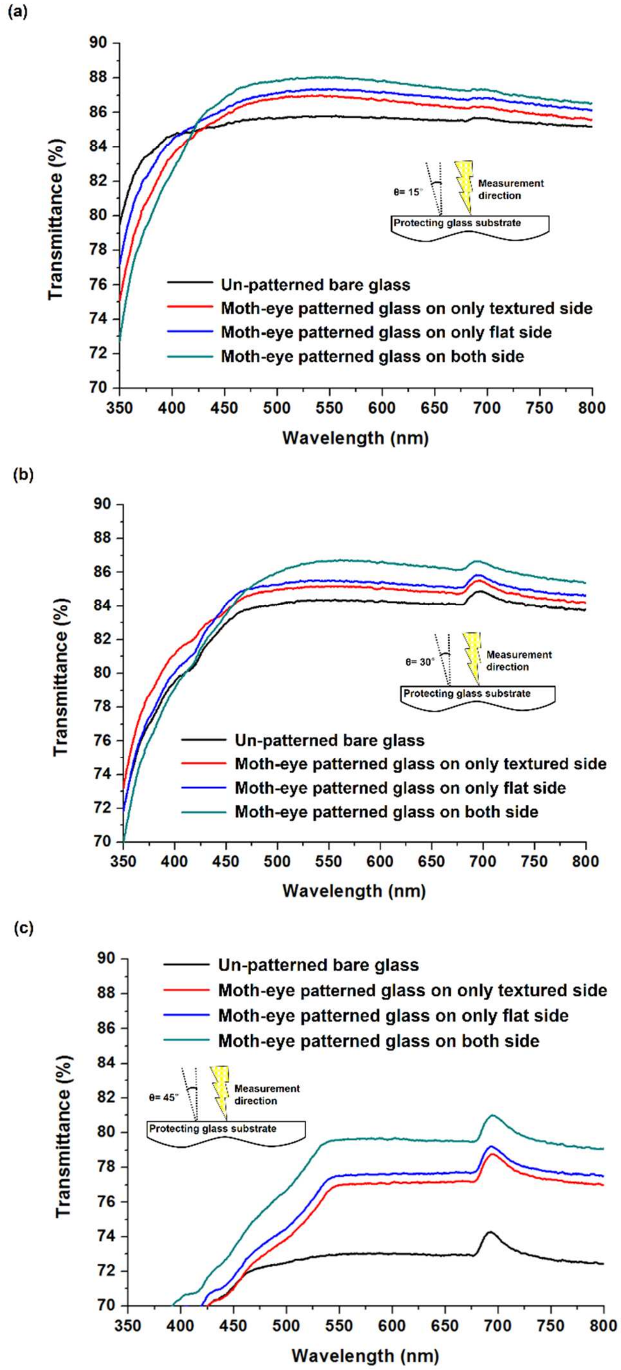

Figure 8. I-V characteristic changes due to PV protective glass with moth-eye patterns

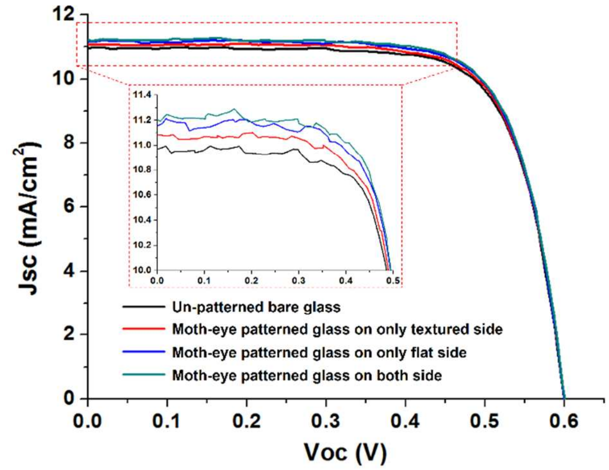

Figure 9. (a) Comparison of the electrical properties of each PV module used in the monitoring system; each module was assembled with un-patterned glass, moth-eye patterned glass on the textured side only, patterned glass on the flat side only and patterned glass on both sides. (b) Schematic structure of PV module with PV protective glass used in field tests.

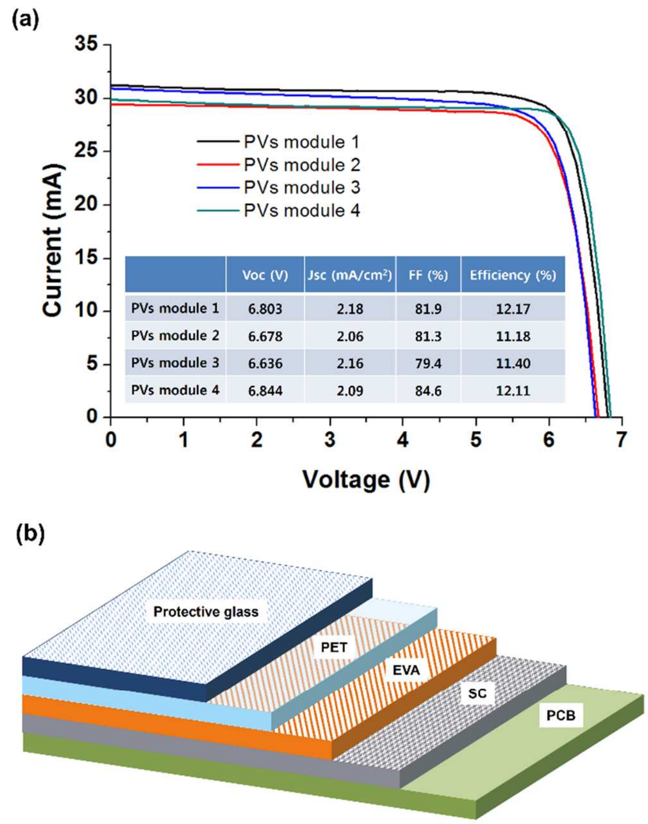

	Voc (V)	Jsc (mA/cm²)	FF (%)	Efficiency (%)
PVs module 1	6.803	2.18	81.9	12.17
PVs module 2	6.678	2.06	81.3	11.18
PVs module 3	6.636	2.16	79.4	11.40
PVs module 4	6.844	2.09	84.6	12.11

Figure 10. Comparison of PV modules with moth-eye patterns: Field test on (a) 04th, 05th, 06th, and 07th Oct. 2013.

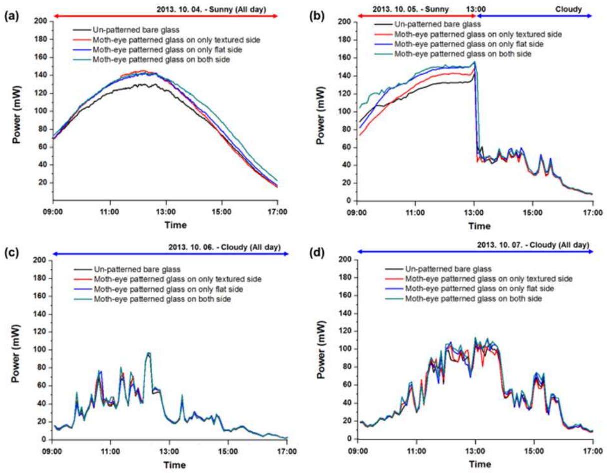

Table 1. Changes in electrical power generated due to moth-eye patterns

Power (mW) \ Date	2013. 10. 04. (Sunny)	2013. 10. 05. (Partially Cloudy)	2013. 10. 06. (Cloudy)	2013. 10. 07. (Cloudy)
Un-patterned bare glass	29430.10 (100%)	7481.86 (100%)	2926.63 (100%)	5006.37 (100%)
Moth-eye patterned glass on only textured side	31251.00 (106.19%)	7511.20 (101.07%)	3013.57 (104.64%)	5130.93 (100.98%)
Moth-eye patterned glass on only flat side	31672.30 (107.62%)	8095.95 (108.94%)	3006.75 (104.53%)	5345.43 (104.41%)
Moth-eye patterned glass on both side	33007.32 (112.16%)	8399.97 (113.03%)	3014.81 (104.83%)	5564.64 (108.43%)

Conclusions

In this study, H-NIL technology was used to enhance the conversion efficiency of PV modules. Moth-eye patterns, a type of anti-reflection layer, were formed on PV protective glass. These moth-eye patterns had a width of 250-350 nm and a height of 233.52 nm and resulted in enhanced optical properties. Transmittance was increased by up to 3.13 % and reflectance decreased by 3.42 %. Furthermore, the transmittance was increased for all incident angles. Due to these enhanced optical properties, the J_{SC} of a single solar cell was increased by up to 3.15 %. Finally, monitoring systems were set up and the total amount of power generated at the module level was enhanced by up to 12.16 %.

Acknowledgements

This research was supported by the Pioneer Research Center Program through the National Research Foundation of Korea funded by the Ministry of Science, ICT & Future Planning (NRF-2013M3C1A3063597) and was supported by Business for Cooperative R&D between Industry, Academy, and Research Institute funded by Korea Small and Medium Business Administration in 2012 (Grant No. C0018361).

Notes and references

[a] Department of Materials Science and Engineering, Korea University, Seoul 136-713, South Korea.
[b] Center for Materials Architecturing, Korea Institute of Science and Technology, Seoul 136-791, South Korea.
[c] Hunetplus, Dusa-ri, Nohsung-myun, Nonsan-si, Chung-nam 320-922 South Korea.

† Footnotes should appear here. These might include comments relevant to but not central to the matter under discussion, limited experimental and spectral data, and crystallographic data.
Electronic Supplementary Information (ESI) available: [details of any supplementary information available should be included here]. See DOI: 10.1039/b000000x/

1 S. Licht, G. Hodes, R. Tnne and J. Manassen, *Nature* 1987, **326**, 863.
2 B. O'Regan and M. Gratzel, *Nature* 1991, **353**, 737.
3 O. Schultz, S.W. Glunz and G.P. Willeke, *Prog. Photovolt: Res. Appl.* 2004, **12**, 553.
4 C.R. Osterwald and T.J. McMahon, *Prog. Photovolt: Res. Appl.* 2009, **17**, 11.
5 G.J. Jorgensen, K.M. Terwilliger, J.A. DelCueto, S.H. Glick, M.D. Kempe, J.W. Pankow, F.J. Pern and T.J. McMahon, *Sol. Energ. Mat. Sol. C.* 2006, **90**, 2739.
6 C.G. Bernhard, *Endeavour* 1967, **26**, 79.
7 S.A. Boden and D.M. Bagnall, *Prog. Photovolt: Res. Appl.* 2010, **18**, 195.
8 N. Yamada, O.N. Kim, T. Tokimitsu, Y. Nakai and H. Masuda, *Prog. Photovolt: Res. Appl.* 2011, **19**, 134.
9 P.B. Clapham and M.C. Hutley, *Nature* 1973, **244**, 281.
10 W.H. Miller, *Ocular Optical Filtering: In Handbook of Sensory Physiology.* Autrum H. ed. 1979, **VII/6A**, 69.
11 P.M. Mendes, S. Jacke, K. Critchley, J. Plaza, Y. Chen, K. Nikitin, R.E. Palmer, J.A. Preece, S.D. Evans and D. Fitzmaurice, *Langmuir* 2004, **20**, 3766.
12 G. Feiertag, W. Ehrfeld, H. Freimuth, H. Kolle, H. Lehr, M. Schmidt, M.M. Sigalas, C.M. Soukoulis, G. Kiriakidis, T. Pedersen, J. Kuhl and W. Koenig, *Appl. Phys. Lett.* 1997, **71**, 1441.
13 F. Stehlin, F. Wieder, A. Spangenberg, J.M. Le Meins and O. Soppera. *J. Mater. Chem. C* 1999, **35**, 694.
14 T.M. Bloomstein, M.F. Marchant, S. Deneault, D.E. Hardy and M. Rothschild, *Opt. Express* 2006, **14**, 6434.
15 S.Y. Chou, P.R. Krauss, W. Zhang, L. Guo and L. Zhuang, *J. Vac. Sci. Technol. B* 1997, **15**, 2897.
16 J.D. Hoff, L.J. Cheng, E. Meyhofer, L.J. Guo and A.J. Hunt, *Nano Lett.* 2004, **4**, 853.
17 L.J. Guo, *Adv. Mater.* 2007, **19**, 495.
18 X. Hu, T. Yang, R. Gu, Y. Cui, C. Yuan, H Ge, W. Wu, W. Li and Y. Chen, *J. Mater. Chem. C* 2014, **2**, 1836
19 J.H. Shin, H.J. Choi, G.T. Kim, J.H. Choi and H. Lee, *Appl. Phys. Express* 2013, **6**, 055001.
20 S.S. Choi, A.S. Lee, S.H. Lee, H.Y. Jeon, K.Y. Baek, D.H. Choi and S.S. Hwang, *J. Polym. Sci. Pol. Chem.* 2011, **49**, 5012.
21 A.S. Lee, S.H. Lee, S.S. Choi, S.H. Lee, H. Y. Jeon, K.Y. Baek and S.S. Hwang, *J. Polym. Sci. Pol. Chem.* 2012, **50**, 4563.
22 R.H. Baney, M. Itoh, A. Sakakibara and T. Suzuki, *Chem. Rev.* 1995, **95**, 1409.
23 W.D. Cook, S. Chen, F. Chen, M.U. Kahveci and Y. Yagci, *J. Polym. Sci. Pol. Chem.* 2009, **47**, 5474.

24 B.W. Johnson and R. McIntyre, *Prog. Org. Coat.* 1996, **27**, 95.
25 K.Y. Yang, S.C. Oh, H.W. Park, H. Lee, *J. Vac. Sci. Technol. B* 2011, **29**, 051602.
26 L. Vogelaar, W. Nijdam, H. Wolferen, R.M. Ridder, F.B. Segerink, E. Fluck, L. Kuipers and N.F. Hulst, *Adv. Mater.* 2001, **13**, 1551.
27 K. Choi, S.H. Park, Y.M. Song, Y.T. Lee, C.K. Hwangbo, H. Yang, H.S. Lee, Adv. Mater. 2010, **22**, 3713.
28 S.H. Hong, B.J. Bae, K.S. Han, E.J. Hong, H. Lee and K.W. Choi, Electron. Mater. Lett. 2009, **5**, 39.

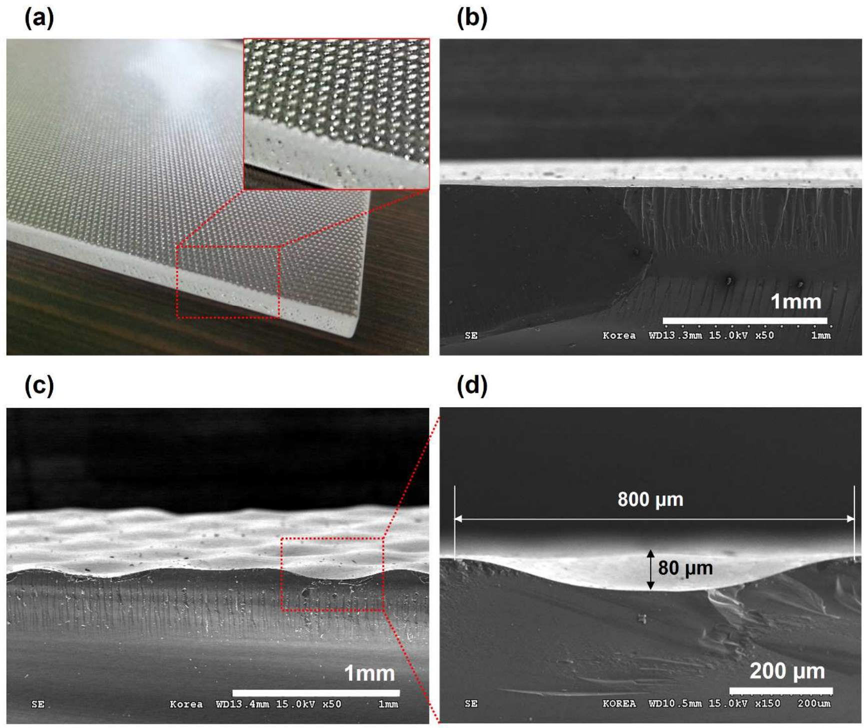

254x190mm (300 x 300 DPI)

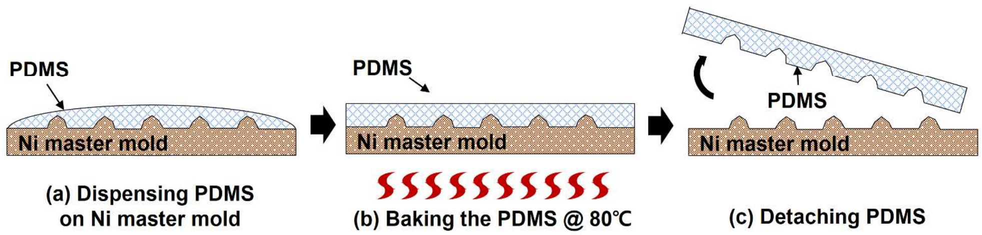

237x58mm (300 x 300 DPI)

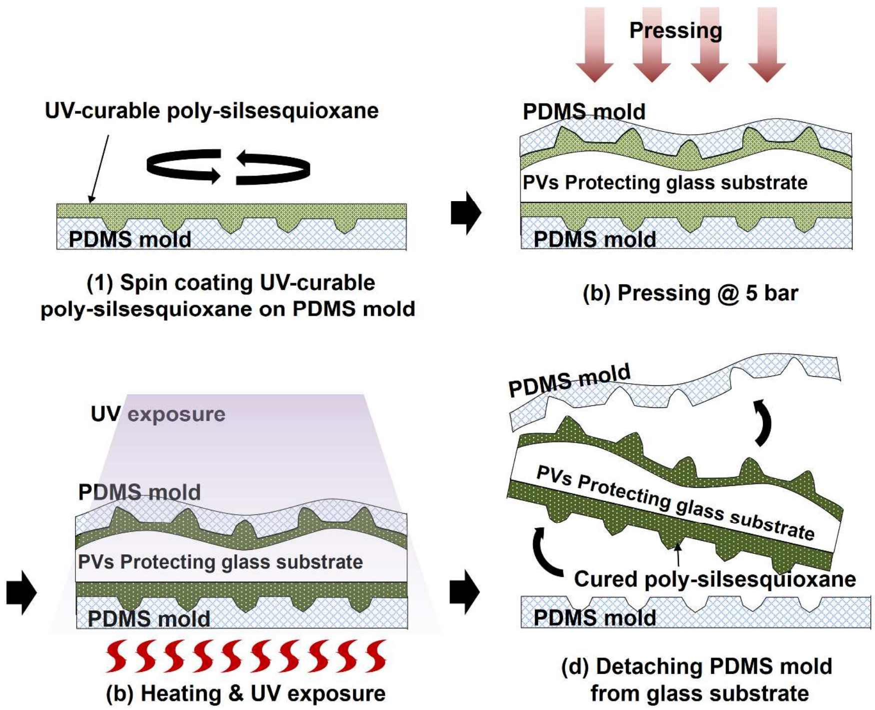

254x190mm (300 x 300 DPI)

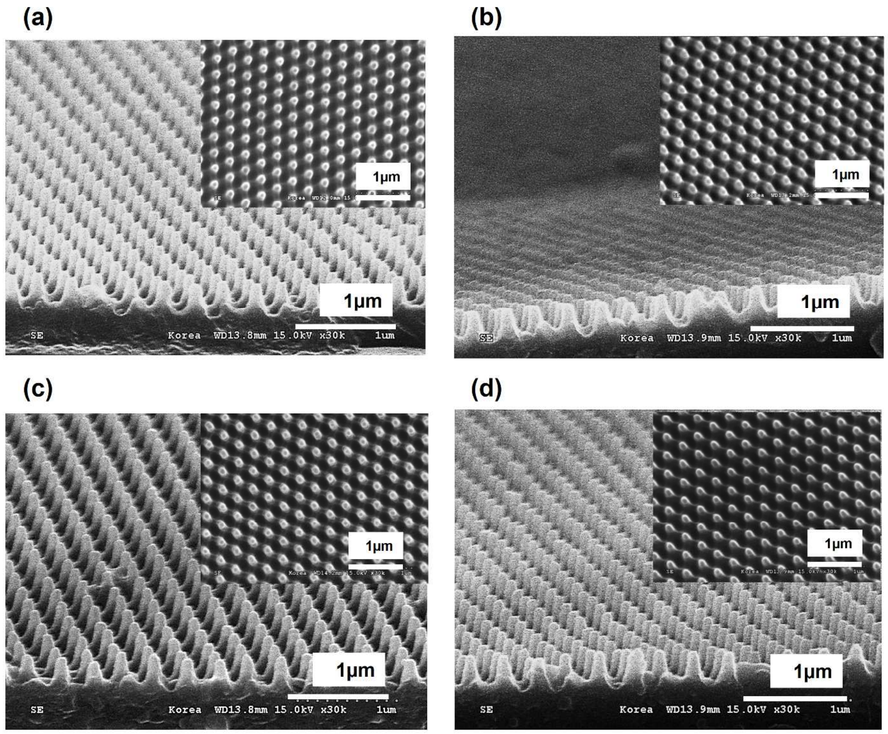

254x190mm (300 x 300 DPI)

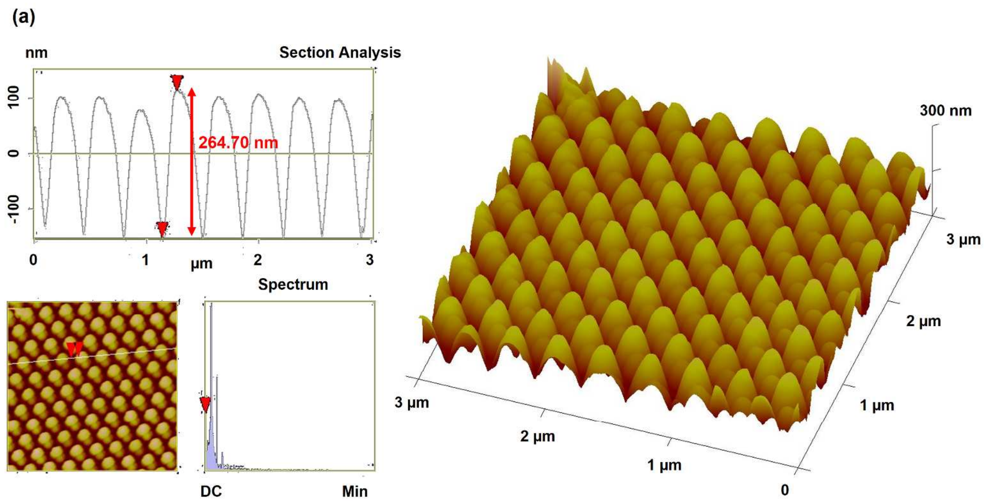

254x190mm (300 x 300 DPI)

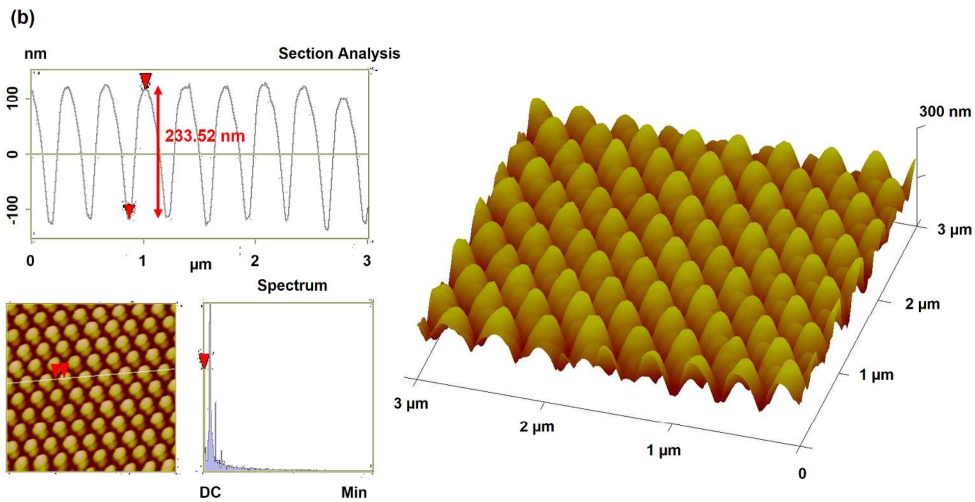

254x190mm (300 x 300 DPI)

(a)

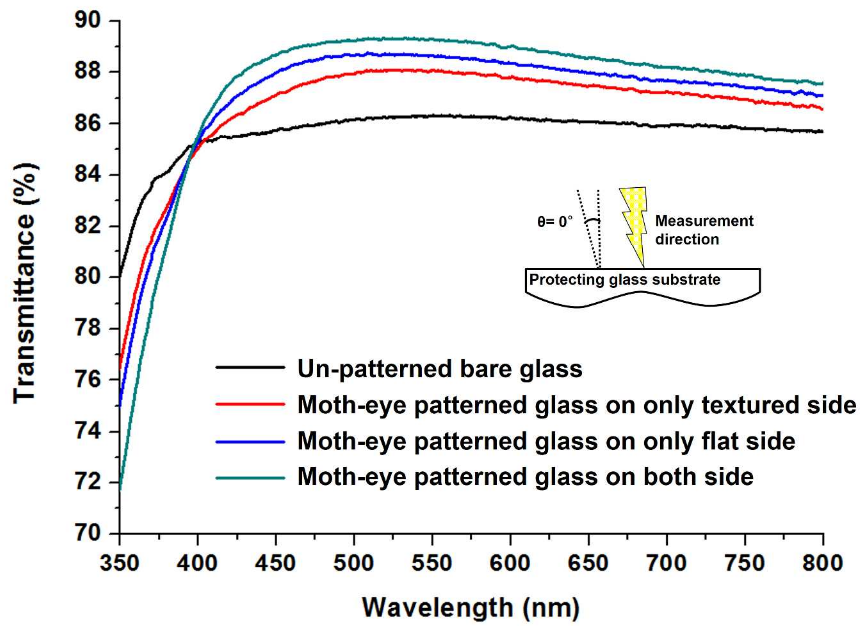

254x190mm (300 x 300 DPI)

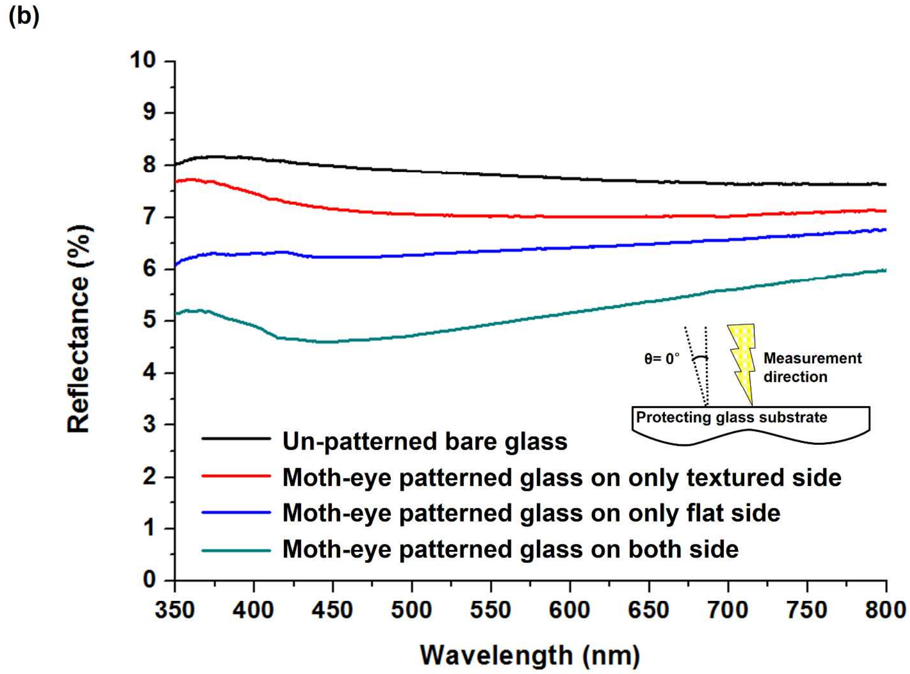

254x190mm (300 x 300 DPI)

(a)

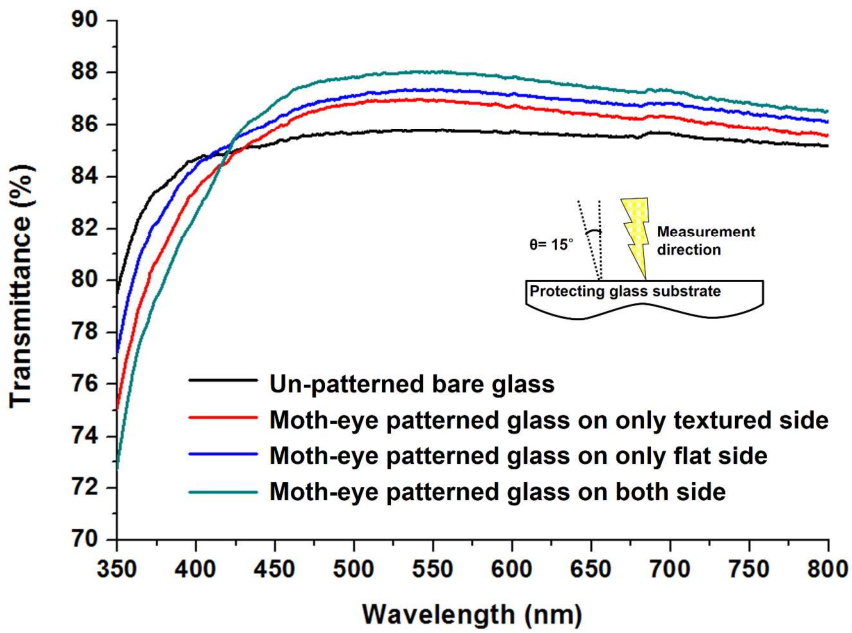

254x190mm (300 x 300 DPI)

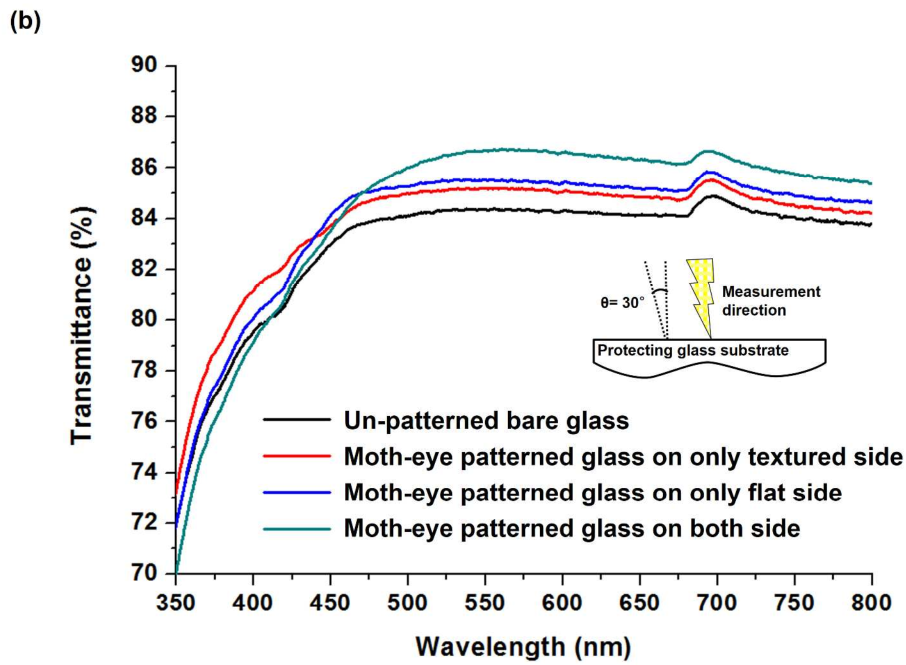

254x190mm (300 x 300 DPI)

(c)

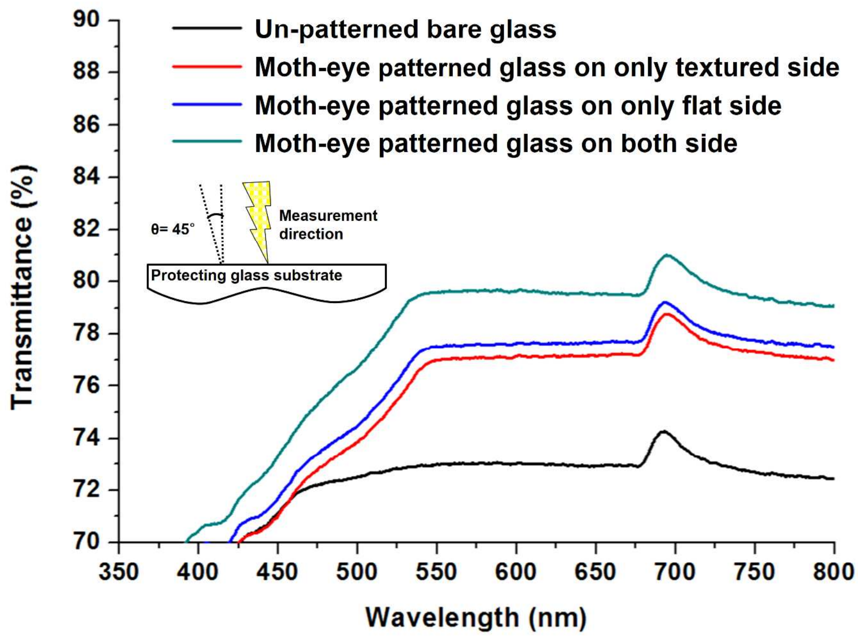

254x190mm (300 x 300 DPI)

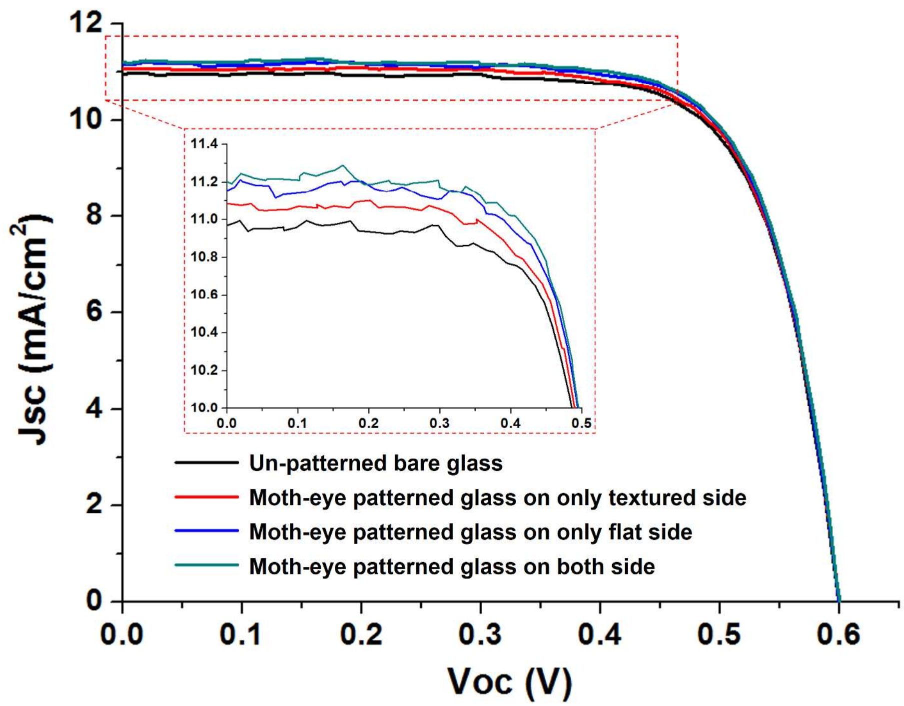

254x190mm (300 x 300 DPI)

(a)

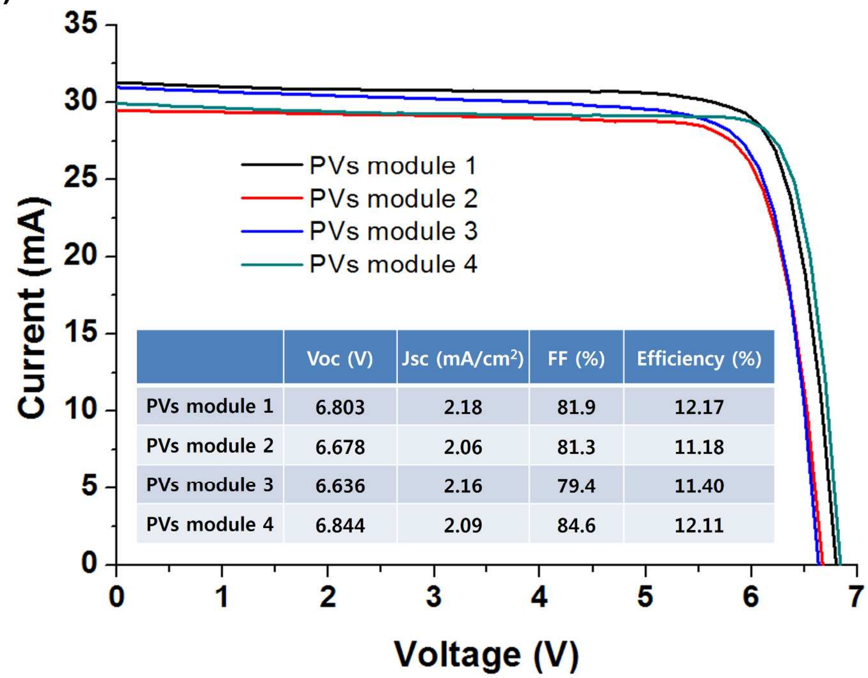

254x190mm (300 x 300 DPI)

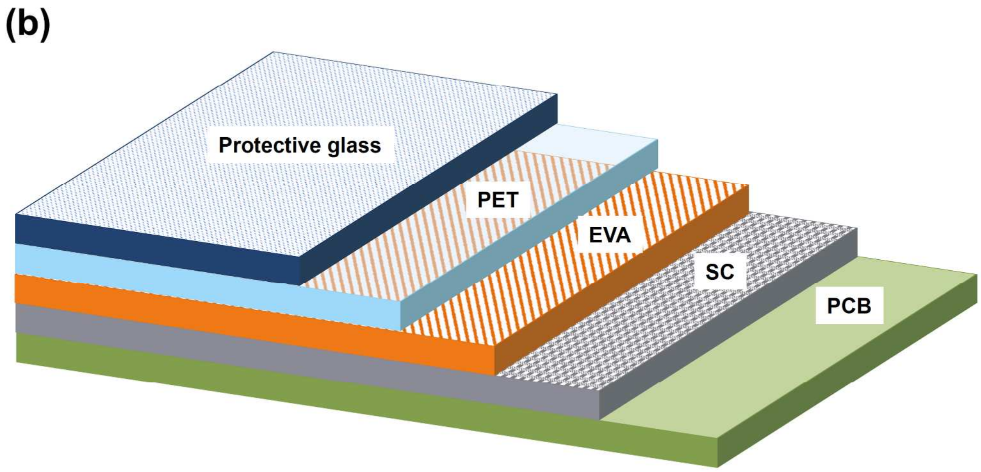

231x114mm (300 x 300 DPI)

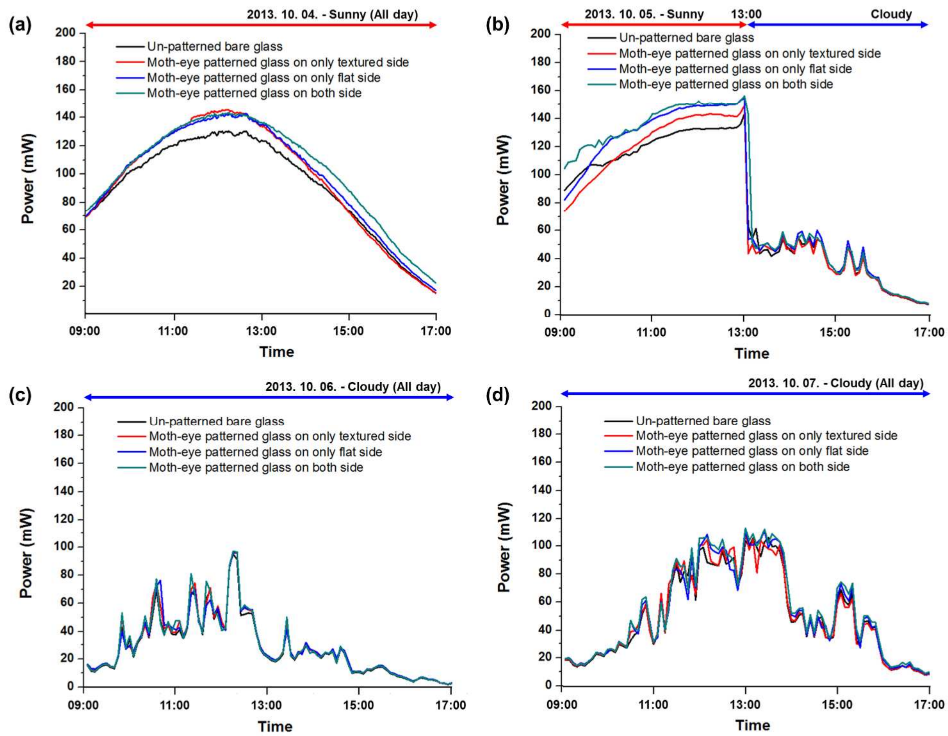

254x190mm (300 x 300 DPI)

Power (mW) \ Date	2013. 10. 04. (Sunny)	2013. 10. 05. (Partially Cloudy)	2013. 10. 06. (Cloudy)	2013. 10. 07. (Cloudy)
Un-patterned bare glass	29430.10 (100%)	7481.86 (100%)	2926.63 (100%)	5006.37 (100%)
Moth-eye patterned glass on only textured side	31251.00 (106.19%)	7511.20 (101.07%)	3013.57 (104.64%)	5130.93 (100.98%)
Moth-eye patterned glass on only flat side	31672.30 (107.62%)	8095.95 (108.94%)	3006.75 (104.53%)	5345.43 (104.41%)
Moth-eye patterned glass on both side	33007.32 (112.16%)	8399.97 (113.03%)	3014.81 (104.83%)	5564.64 (108.43%)

234x83mm (300 x 300 DPI)

Graphical abstract

Fabrication of functional nano-sized patterns with UV-curable polysilsesquioxane on photovoltaic protective glass substrates using hybrid nano-imprint lithography

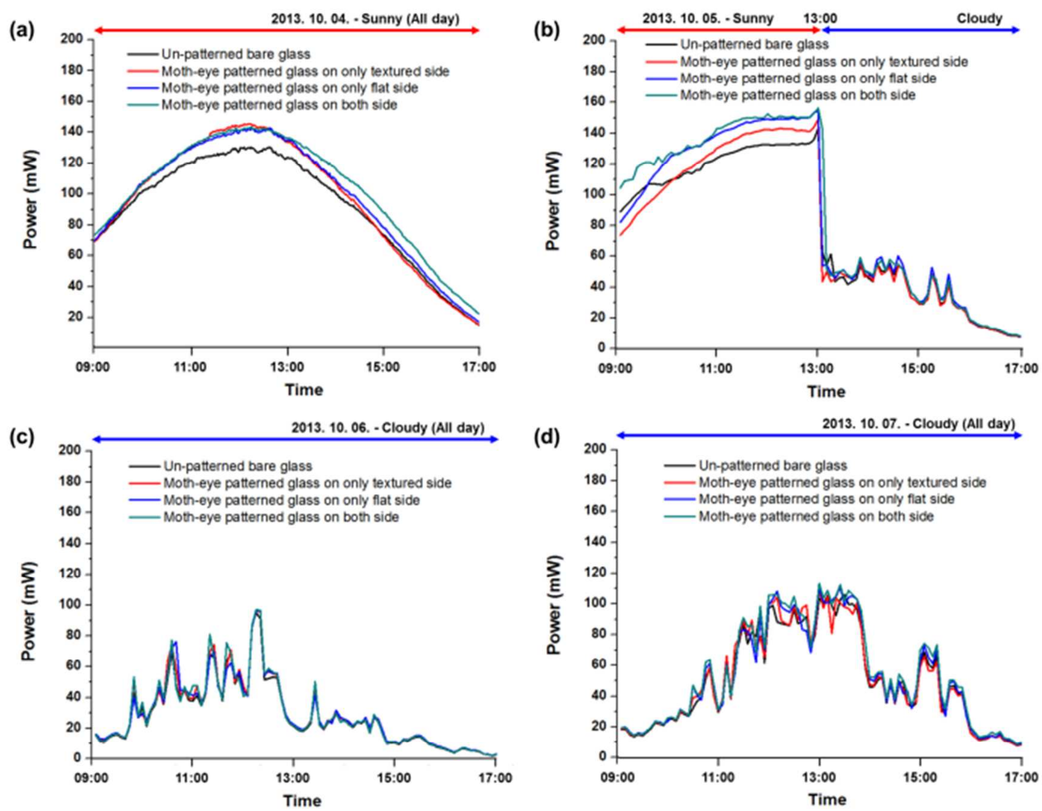

Ju-Hyeon Shin (Heon Lee*) fabricated moth-eye structures on photovoltaic (PV) protective glass a hybrid nano-imprint lithography technique. The efficiency of the PV module with PV protective glass patterned on both sides was enhanced by up to 12.16% compared to that of the PV module with un-patterned PV protective glass.